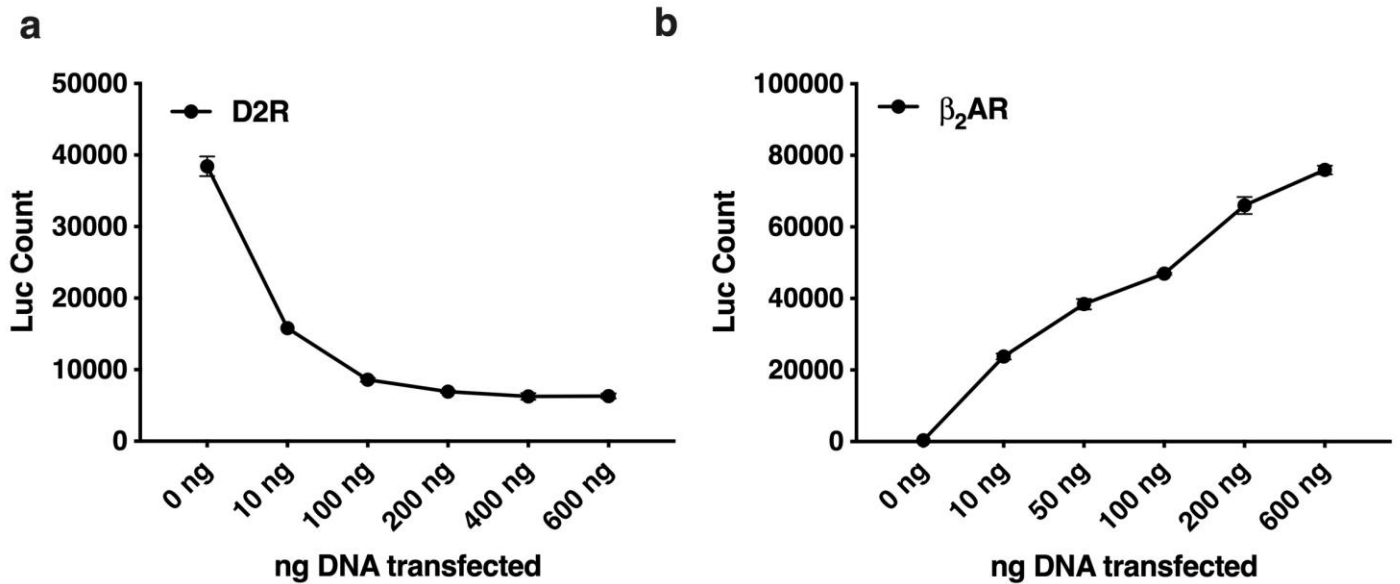
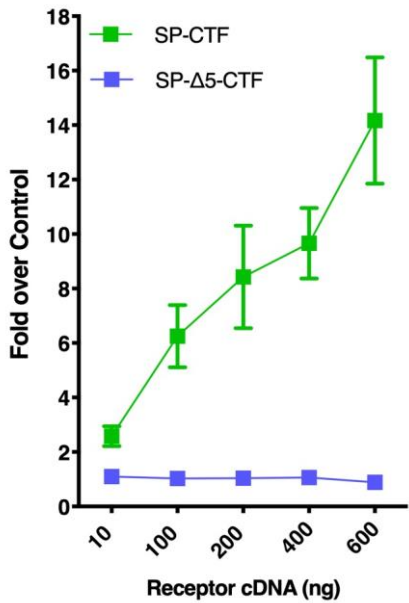


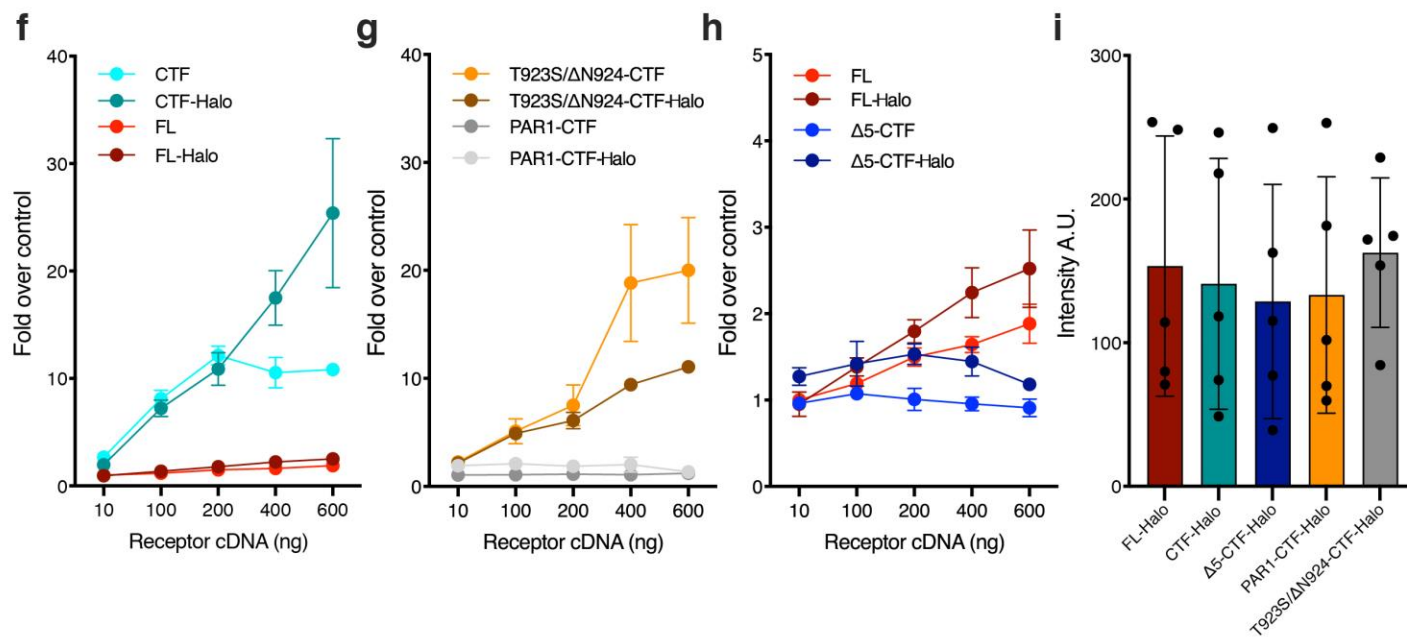
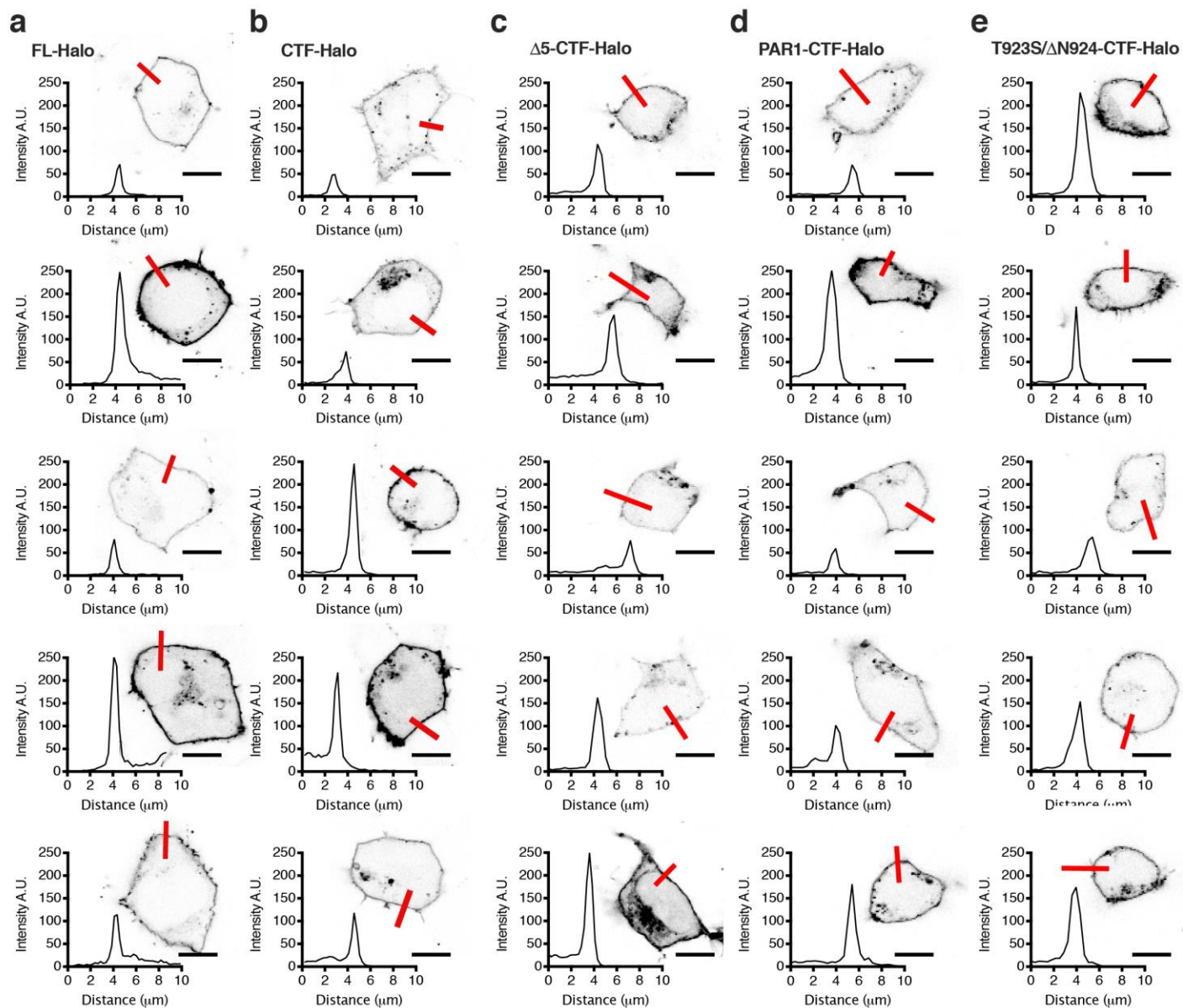
Supplementary Figures



Supplementary Fig. 1. Controls for constitutive activity of two well-characterized Gs and Gi/o coupled receptors in the CRE gene expression assay. (a) D2R (Gi, cAMP \downarrow) and (b) β_2 AR (Gs, cAMP \uparrow). Luminescence was measured for a range of increased receptor cDNA concentrations ~24 hours after transfection in HEK293T cells. In (b) cells were stimulated by 30 μ M forskolin for 6 hours prior to luminescence reading. Data from one representative experiment performed 4 (a) and 5 (b) times. Data are presented as mean \pm SD from triplicate 96-well replicates.

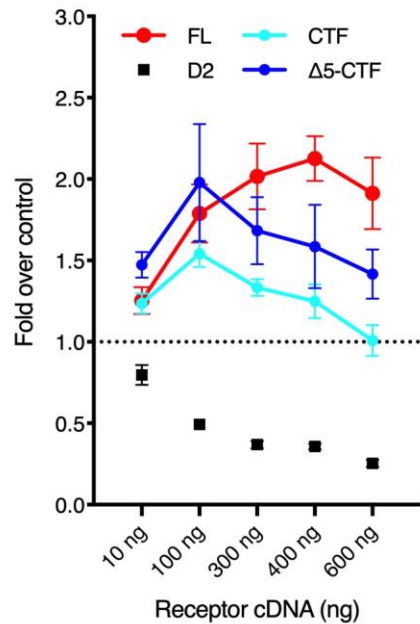


Supplementary Fig. 2. Evaluating the effect of the Adgr13 endogenous signal peptide in the CTF and Δ5-CTF constructs. The TA in the CTF construct only differs from the TA that would be exposed *in vivo* by the N-terminal methionine residue that is translated from the repositioned start codon (**Fig. 1b**). We tested the effect of adding the Adgr13 signal peptide to the N terminus of CTF (SP-CTF) and Δ5-CTF (SP-Δ5-CTF). We found that SP-CTF and SP-Δ5-CTF had CRE activity comparable to that of CTF and Δ5-CTF in **Fig. 1c** suggesting that they function similarly. We therefore used the CTF and Δ5-CTF constructs that lack the signal peptide for all subsequent analysis in order to be certain of the exact starting sequence without a need to validate SP cleavage. Luminescence was measured for a range of receptor cDNA concentrations ~24 hours after transfection in HEK293T cells. All data points are normalized to empty vector control. Data represent mean \pm SEM from 6 independent experimental replicates.



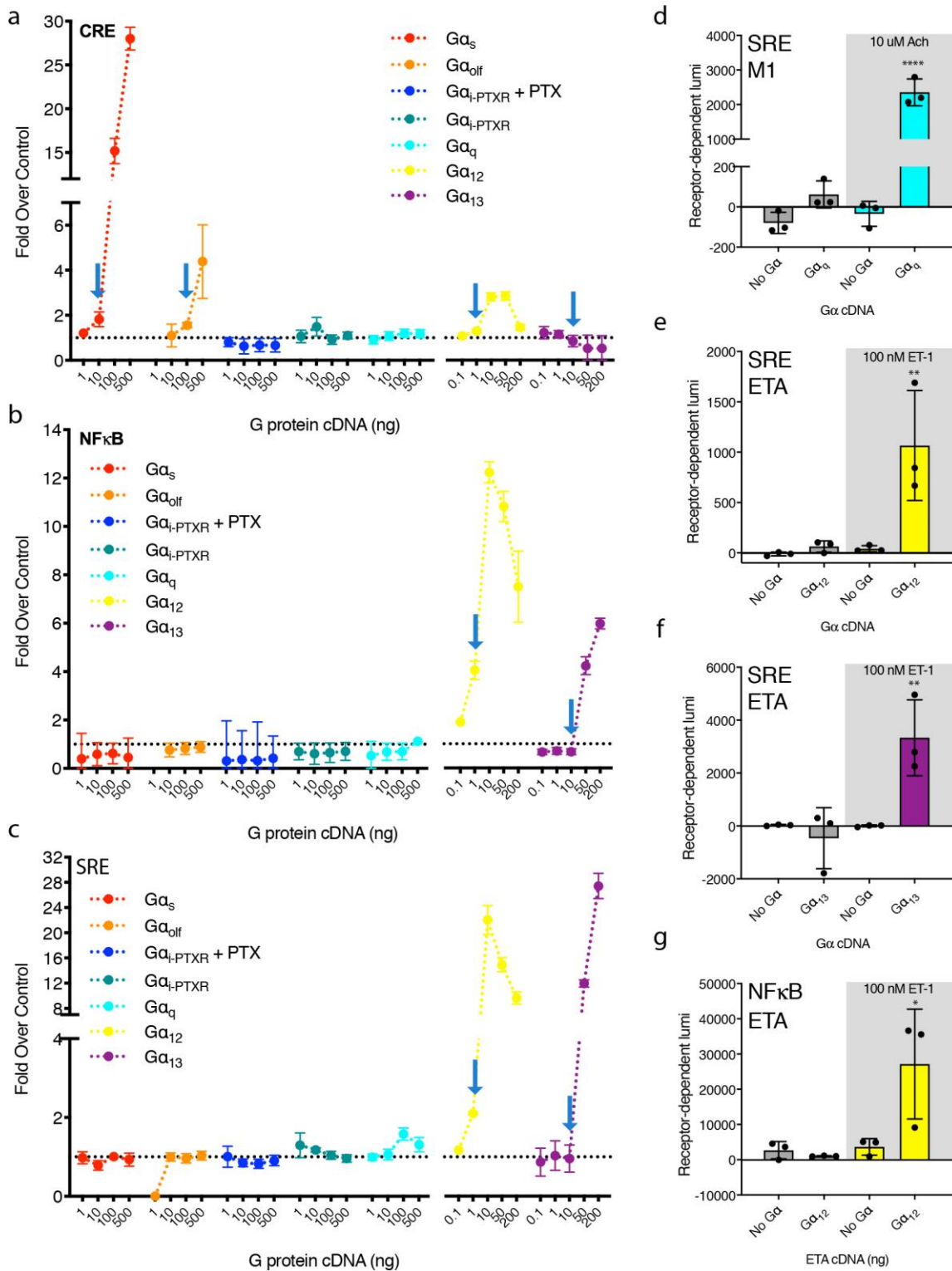
Supplementary Fig. 3. FL and CTF receptor constructs are expressed at the cell surface at comparable levels.

Micrographs of 5 HEK293T cells transiently expressing (a) FL-Halo (b) CTF-Halo (c) Δ 5-CTF-Halo (d) Par1-CTF-Halo or (e) T923S/ Δ N924-CTF-Halo labelled by the Janelia fluorophore JF-646. Line scans marked by red line (5 pixels wide) and corresponding intensity profiles are shown below each cell. All cells were imaged by confocal microscopy employing identical imaging settings for gain, line scanning, zoom, and laser line intensity (640 nm). In (a-e) 5 representative cells collected in 2 independent experiments are shown. Scalebar 10 μ M (black lines). (f) CRE gene expression assay showing that the C-terminally Halo-tagged receptor constructs function similarly to FL and CTF constructs. (g) CRE gene expression assay showing that the C-terminally Halo-tagged PAR1 chimeric constructs function similarly to the PAR1-CTF and T923S/ Δ N924-CTF constructs. (h) CRE gene expression assay showing that the C-terminally Halo-tagged Δ 5-CTF-Halo functions similarly to the Δ 5-CTF. For (g-h) luminescence was measured for a range of receptor cDNA concentrations ~24 hours after transfection in HEK293T cells. All data points are normalized to an empty vector control. Data are presented as mean \pm SEM from 3 independent experimental replicates. (i) Bar graph showing average peak intensities from the linescans in (a-e). Bars in (i) show mean \pm SD of the peak intensities for the 5 cells in a-e respectively.



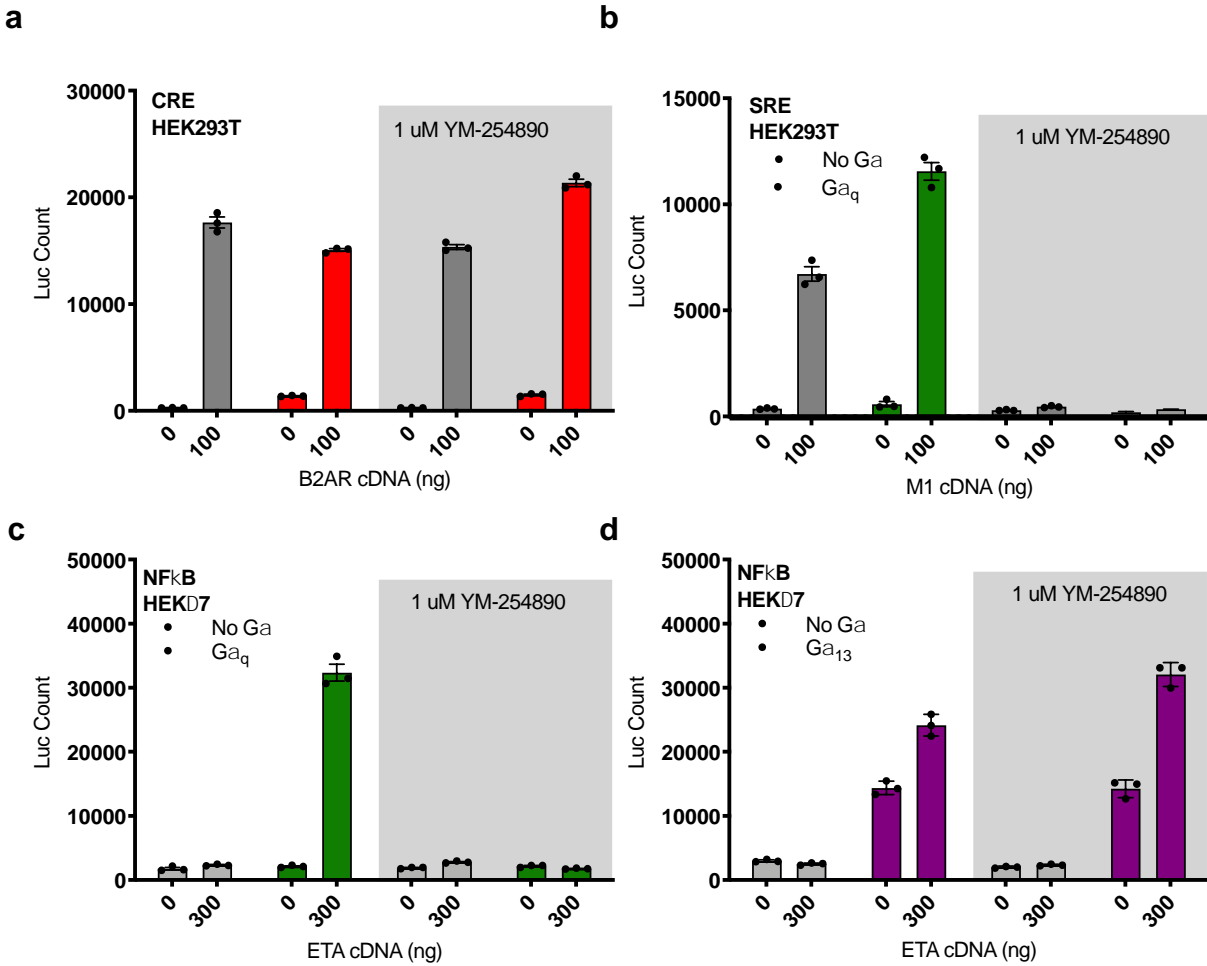
Supplementary Fig. 4. Adgrl3 constructs do not inhibit cAMP in the CRE gene expression assay in HEK Δ 7 cells. (a)

Gene expression assay for FL, CTF, $\Delta 5$ -CTF, and control D2R. Adenylyl cyclase requires $G\alpha_s$ to raise cAMP in response to forskolin^{1,2}. In the HEK Δ 7 (that is devoid of $G\alpha_s$) we therefore raised cAMP with forskolin (50 μ M) and by co-transfecting a truncated $G\alpha_s$ lacking the last ten amino acids of the C terminus ($G\alpha_{s\Delta 10}$, 160 ng), which has been shown to abolish β_2 AR coupling, but still work to complement adenylyl cyclase activity. Luminescence signals were evaluated for empty vector control and receptor constructs ~24 hours after transfection. All data points are normalized to the corresponding empty vector control. Data are presented as mean \pm SEM from 3 independent experimental replicates.

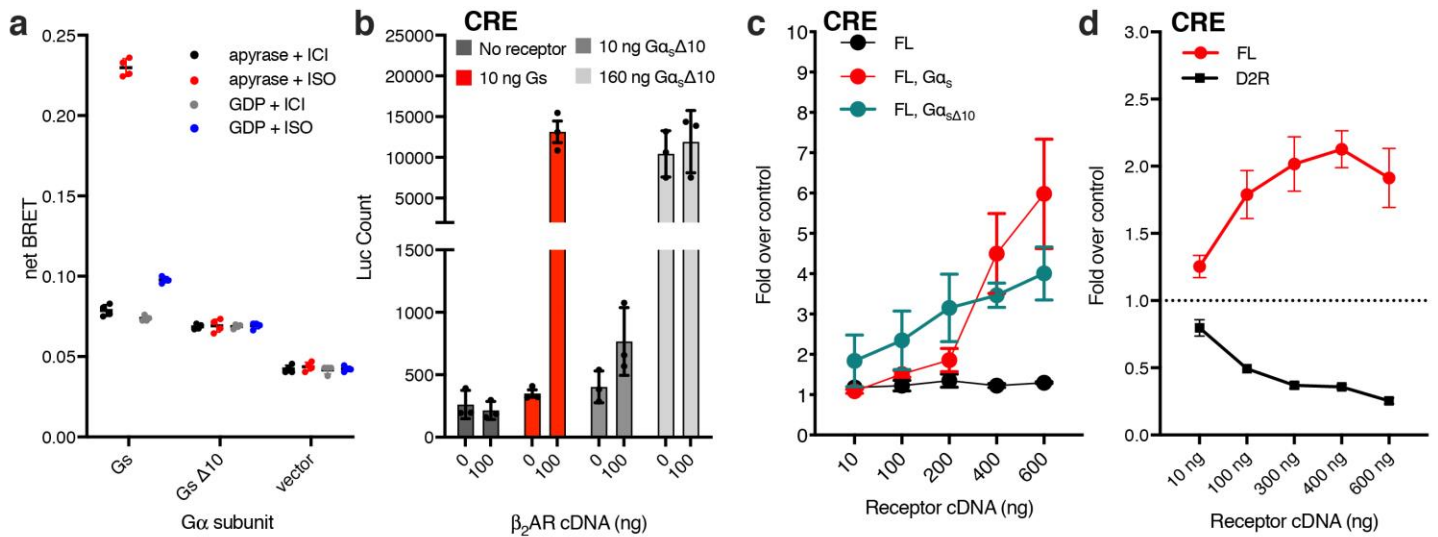


Supplementary Fig. 5. HEK Δ 7 G α subunit assay optimization. The HEK Δ 7 CRISPR knockout cell line lacks the main G protein families $G\alpha_s/G\alpha_{olf}$, $G\alpha_z$, $G\alpha_q/G\alpha_{11}$ and $G\alpha_{12}/G\alpha_{13}$. **(a-c)** Titrations of cDNA for each G α subunit in three different gene expression assays (CRE, NF κ B, and SRE). Blue arrows mark the concentrations used in the actual screens. For $G\alpha_q$

and $G\alpha_{i-PTXR}$, 200 ng was used. **(a-c)** All data points are normalized to the corresponding empty vector control. **(d-f)** Controls showing that M1 signals in SRE only with $G\alpha_q$ reintroduced and that ETA signals in SRE only with $G\alpha_{12/13}$ reintroduced. **(g)** Control showing that ETA signals in NF κ B only with $G\alpha_{12}$ reintroduced. **(d-g)** Each $G\alpha$ protein species was reintroduced one at a time (see color legend for specification) at optimized cDNA concentrations and luminescence signals were evaluated for empty vector control and receptor constructs ~24 hours after transfection. For conditions marked by a grey box in **(d-g)**, Ach or ET-1 agonist concentration was maintained at 10 μ M or 100 nM respectively for 5 hours before reading the luminescence signal. Data are presented as mean \pm SEM from 3 independent experimental replicates. In panels **(d-g)** the baseline signal of empty vector is subtracted to show receptor-dependent luminescence (lumi). One-way ANOVA with Tukey's multiple-comparison post-hoc test was performed to determine statistical significance between the four conditions in each panel (**d**, **** $p < 0.0001$) (**e**, ** 'No $G\alpha$ ' vs. ' $G\alpha_{12}/ET1$ ' $p = 0.0059$, $G\alpha_{12}$ vs. ' $G\alpha_{12}/ET1$ ' $p = 0.0091$, 'No $G\alpha/ET1$ ' vs. ' $G\alpha_{12}/ET1$ ' $p = 0.0080$) (**f**, ** 'No $G\alpha$ ' vs. ' $G\alpha_{13}/ET1$ ' $p = 0.0099$, $G\alpha_{13}$ vs. ' $G\alpha_{13}/ET1$ ' $p = 0.0043$, 'No $G\alpha/ET1$ ' vs. ' $G\alpha_{13}/ET1$ ' $p = 0.0094$) (**g**, 'No $G\alpha$ ' vs. ' $G\alpha_{12}/ET1$ ' $p = 0.0232$, $G\alpha_{12}$ vs. ' $G\alpha_{12}/ET1$ ' $p = 0.0164$, 'No $G\alpha/ET1$ ' vs. ' $G\alpha_{12}/ET1$ ' $p = 0.0284$). See also Supplementary Data for the full set of p -values and test details.

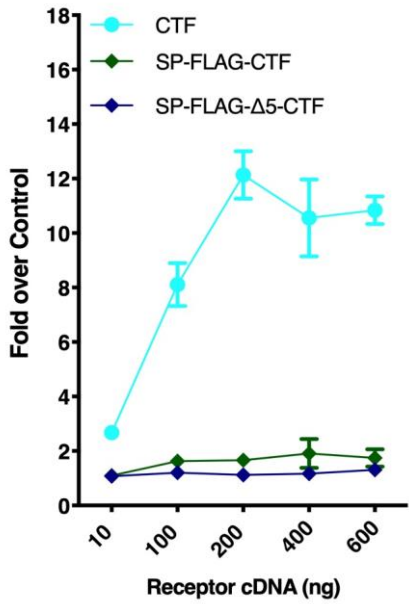


Supplementary Fig. 6. $G\alpha_q$ inhibitor (YM-254890) controls. (a) YM-254890 had no effect on β_2AR ($G\alpha_s$ coupled) constitutive activity in CRE. (b) YM-254890 inhibited M1 ($G\alpha_q$ coupled) signaling in SRE. To dissect the effect of YM-254890 in NF κ B for $G\alpha_q$ and $G\alpha_{13}$ signaling, we had to use the HEK Δ 7 cell line because receptors that couple to $G\alpha_{13}$ also couple to other $G\alpha$'s. We used ETA as a control receptor as it couples to $G\alpha_q$ and $G\alpha_{12/13}$. (c) YM-254890 inhibits ETA $G\alpha_q$ signaling. (d) YM-254890 has no effect on ETA $G\alpha_{13}$ signaling. Luminescence signals are evaluated for empty vector control and receptor constructs ~24 hours after transfection. 6 hours before reading media was exchanged with either vehicle (buffer) or 1 μ M YM-254890. For conditions in (b-d) Ach (b) or ET-1 (c-d) agonist concentration was maintained at 10 μ M or 100 nM, respectively, for 6 hours before reading the luminescence signal. Data in **a-d** are from one representative experiment performed twice. Bars indicate mean \pm SD from three 96-well replicates.



Supplementary Fig. 7. FL receptor raised CRE without direct coupling to G α_s . (a) Truncating the last ten amino acids of the G α_s C terminus (construct called G $\alpha_{s\Delta 10}$) abolished β_2 AR coupling. Bioluminescence resonance energy transfer (BRET) between luciferase-tagged β_2 AR and Venus-tagged heterotrimers incorporating G α_s but not G $\alpha_{s\Delta 10}$ was enhanced by agonist stimulation (10 μ M isoproterenol; ISO); baseline BRET was measured in the presence of the inverse agonist ICI 155,181 (ICI; 10 μ M). Experiments were carried out in permeabilized cells lacking endogenous G α_s -family subunits (HEK Δ Gs), which were either treated with apyrase to remove residual nucleotides or supplemented with 100 μ M GDP. (b) G $\alpha_{s\Delta 10}$ complements adenylyl cyclase activity. CRE Gene expression assay controls in HEK Δ 7 cells showing that β_2 AR only signaled to CRE in the presence of 10 ng wt G α_s but not 10 ng G $\alpha_{s\Delta 10}$; at high levels of G $\alpha_{s\Delta 10}$ (160ng) this construct functioned to raise cAMP but the levels were unaffected by co-transfection of β_2 AR. (c) CRE Gene expression assay for FL \pm G α_s or G $\alpha_{s\Delta 10}$ in HEK Δ 7 cells (d) CRE Gene expression assay for Adgrl3 FL and D2R receptors in HEK Δ 7 cells. cAMP was raised with 50 μ M forskolin and 160 ng G $\alpha_{s\Delta 10}$ as described in **Supplementary Fig. 4**. Without G α_s co-expression, FL receptor showed no signal at any of the concentrations explored, but we observed a density dependent increase in CRE when G α_s was co-transfected. It is important to note that adenylyl cyclase is dependent on G α_s/α_{off} for its activation by forskolin^{1,2}. Thus, forskolin has no effect in the CRE assay in the HEK Δ 7 cell line since it lacks both G α_s and G α_{off} . This creates a problem in interpreting the data in **c** as the FL CRE signal is absent without G α_s co-expression. Thus, co-expression of G α_s might “enable” another pathway to adenylyl cyclase activation, thereby leading to CRE signal without direct activation of Gs by FL. To resolve this conundrum and to test if Adgrl3 FL is engaged in direct activation of G α_s , we used the G $\alpha_{s\Delta 10}$ construct. With co-expression of G $\alpha_{s\Delta 10}$ (both with (c) and without forskolin (d)) FL still produced a density-dependent increase in CRE response in the HEK Δ 7, and we therefore conclude that direct Gs activation is not necessary

for the FL effect on CRE in the presence of Gs, since it occurs similarly with $G_{\alpha_{s\Delta 10}}$, which can enable AC activity without coupling to any GPCR. Data points in **(c and d)** are normalized to empty vector control. For **(a)** data are shown as mean \pm SD from 4 independent experiments. For **(a, b and d)** Data are shown as mean \pm SEM from 3 independent experimental replicates.



Supplementary Fig. 8. An N-terminal FLAG tag inhibits TA-enhanced signaling. Adding a FLAG tag in front of CTF dramatically impairs CRE activity. Data points are normalized to empty vector control. Data are presented as mean \pm SEM from 3 independent experimental replicates.

Name	Mutations/Truncations	Description	References
FL		Endogenous Adgrl3 signal peptide and FLAG tag in front of full length Adgrl3	
CTF	Truncated after L922	Adgrl3 truncated at GPS cleavage site to expose the full TA. Methionine is included in front of TA	
$\Delta 5$ -CTF	Truncated after V927	First 5 aa subsequent to GPS cleavage site removed. Methionine is included in front of TA	
$\Delta 3$ -CTF	Truncated after F925	First 3 aa subsequent to GPS cleavage site removed. Methionine is included in front of TA	
F925A-CTF	Alanine substitution F925A in CTF		
F925A-M929A-CTF	Alanine substitutions F925A and M929A in CTF		
SP-CTF		Endogenous Adgrl3 signal peptide in front of TA in CTF construct	
SP- $\Delta 5$ -CTF		Endogenous Adgrl3 signal peptide in front of $\Delta 5$ -CTF construct	
SP-FLAG-CTF		Endogenous Adgrl3 signal peptide and FLAG tag in front of the CTF construct	
SP-FLAG- $\Delta 5$ -CTF		Endogenous Adgrl3 signal peptide and FLAG tag in front of the $\Delta 5$ -CTF construct	
CTF-Halo		Halo tag is fused to the extreme c-terminus of the CTF construct	
FL-Halo		Halo tag is fused to the extreme c-terminus of the FL construct	
PAR1-CTF		Endogenous Par1 signal peptide and N-terminal region up to the cleavage site LDPR/SF is fused to the Adgrl3 CTF construct	
T923S/ Δ N924-CTF		M-SFAVLM-CTF. Control construct exposing the TA (M-SFAVLM) produced after thrombin cleavage of PAR1-CTF construct. Methionine is included in front of TA	
G α_{13} -Halo		Human G α_{13} with Halo inserted at position 128	3
G α_{i1} -Halo		Human G α_{i1} with Halo inserted at position 91	4
G α_{i1} -Halo-PTXR		Human G α_{i1} with Halo inserted at position 91. Pertussis toxin-resistant version.	
$\Delta 5$ -CTF-Halo		Halo tag is fused to the extreme C-terminus of the $\Delta 5$ -CTF construct	
PAR1-CTF-Halo		Halo tag is fused to the extreme C-terminus of the PAR1-CTF construct	
T923S/ Δ N924-CTF-Halo		Halo tag is fused to the extreme C-terminus of the T923S/ Δ N924-CTF construct	

Supplementary Table 1. Novel cDNA constructs used in this study. For the G α_{13} -Halo construct Halo was inserted at position 128 in the same position as mTurquoise2 was introduced previously³. For the G α_{i1} -Halo / G α_{i1} PTXR constructs Halo was inserted at position 91 in the same position as luciferase was introduced previously⁴.

1. Green, D.A. & Clark, R.B. Direct evidence for the role of the coupling proteins in forskolin activation of adenylate cyclase. *J Cyclic Nucleotide Res* **8**, 337-346 (1982).
2. Downs, R.W., Jr. & Aurbach, G.D. The effects of forskolin on adenylate cyclase in S49 wild type and cyc-cells. *J Cyclic Nucleotide Res* **8**, 235-242 (1982).
3. Mastop, M., Reinhard, N.R., Zuconelli, C.R., Terwey, F., Gadella, T.W.J., Jr., van Unen, J., Adjobo-Hermans, M.J.W. & Goedhart, J. A FRET-based biosensor for measuring Galpha13 activation in single cells. *Plos One* **13**, e0193705 (2018).
4. Gales, C., Van Durm, J.J., Schaak, S., Pontier, S., Percherancier, Y., Audet, M., Paris, H. & Bouvier, M. Probing the activation-promoted structural rearrangements in preassembled receptor-G protein complexes. *Nat Struct Mol Biol* **13**, 778-786 (2006).